"Studies of rain erosion mechanisms in a range of I.R. transmitting ceramics including coated samples"

1. INTRODUCTION

The report starts by summarising the techniques and approaches used in this laboratory to study liquid impact, rain erosion damage mechanisms and the strength properties of "window" materials. Recent progress is then discussed. This includes (i) a recalibration, and extension to lower velocities of the "equivalent drop size" data for the impact of jets from the Cambridge single impact apparatus (ii) a summary of recent work on zinc sulphide, including the work on various coated systems covered by Purchase Order F6170887W0948.

1.1. Liquid Impact Apparatus

The Cambridge group has pioneered the technique by which a liquid jet is fired against a stationery target. However, facilities are also available for projecting specimens of up to 25.4 mm diameter against stationary drops. The first has distinct advantages in its ease of operation, low construction cost, and the velocity range which can be covered. The second is nearer the practical situation, since a spherical drop is struck, but has disadvantages as regards the size of specimen which can be projected and the deceleration (without further damage) of the specimen after impact. The suspension of spherical drops of diameter greater than 2 mm is also a problem.

The liquid jet method has, over the years, been placed on a sounder quantitative basis and it is now possible to relate jet impact at a certain velocity with an "equivalent" drop size (see, for example, Field et al. 1979, 1983, Hand, 1987).

In a third type of experiment, techniques have been developed for impacting two-dimensional drops and wedges of gelatine. This approach allows processes occurring inside the drop (for example, shock waves, cavitation) and the onset of jetting to be studied in detail. It is also closer to situations which can be evaluated analytically (see, for example, Field, Lesser and Dear 1985).

The jet method can be used to study multiple impact, but this means reloading the chamber with liquid and repressurising the gun. This process becomes tedious if more than say, 10 impacts have to be made on one spot. Other techniques for producing multiple impact (rotating arm, wheel and jet, rocket sledge) are usually expensive to construct and to operate. It was recognised a few years ago that it would be advantageous to have a jet impact apparatus which could impact a specimen with a sequence of controlled jets. A multiple impact jet apparatus (MIJA) has since been developed and is now in regular use for rain erosion studies (Davies and Field 1987).

1.2 Residual strength curves and equivalent flaw sizes

Since the early 1970s, we have placed damage assessment on a sounder basis by measuring post-impact "residual" strengths. This involves impacting a specimen under known conditions and then measuring the strength. Curves of "residual" strength versus impact velocity give a clear indication of the threshold velocity range for damage and how subsequently the strength degrades with higher velocities of impact. A hydraulic apparatus which stresses disc specimens has been developed for this work (Gorham & Rickerby, 1975, Matthewson & Field, 1980). This method has the advantage of keeping "edge" failures to a minimum since only the central regions of the disc have high tensile stress applied. This quantitative assessment of damage is one of the main features of our work.

In practice, a disc shaped specimen is impacted at its centre at a chosen velocity. It is then placed in the hydraulic pressure tester, and stressed to failure. The impacted face is the one subjected to tensile loading. In general, specimens which fail at a low load fracture into a few pieces while those that fail at high loads fracture into many. It is usually possible to locate the fracture origin and the angular orientation of the initiating defect from which it grew. The origin is not necessarily at the centre of the disc where the stresses are greatest because the main defect may be non-central. The fracture stress at the defect can be calculated from the measured failure load and the position and orientation of the initiating defect.

If the fracture toughness, K_{Ic}, of the material is known it is possible to work out an "equivalent flaw size" (e.f.s) for the initiating defect. The equivalent flaw is assumed to have a simple half-penny shape.

Residual strength curves usually have an initial plateau value up to a "threshold velocity". It is not until the threshold is exceeded that the impact stresses are sufficient to propagate the material's inherent defects. It is worth emphasizing that "visible" damage usually only appears at a significantly higher velocity than that located by residual strength measurements. This is because even when the threshold is exceeded, and the strength has dropped, the defects may still be submicroscopic.

The site of the initiating defect in the hydraulic test can give useful information. If it forms away from the impact site, for impact velocities above the threshold, it suggests that a large defect (usually grinding damage) existed at that point.

There is, of course, a statistical spread of results as would be expected with all brittle materials. The spread in strength values for a particular loading condition is a good indication of the quality of the material and its surface preparation.

If a specimen survives one impact undamaged it usually survives further impacts. This is because the pulse duration from a liquid impact is very short and stress corrosion effects are not possible.

However, multiple impacts at above threshold values continue to extend the defects. This has the effect of sharpening the step in the residual strength curve at the

threshold value. In practice, we usually impact 5 times on the same spot before loading in the hydraulic test.

The loss in strength after an above-threshold impact is usually by a finite amount since the defect growth is limited by the short duration of the impact.

1.3 High-speed photograph

Great use has been made at Cambridge of high-speed photography for studies of (a) jet production, (b) jetting and flow phenomena following impact, (c) stress produced by impact, and (d) damage initiation and propagation.

1.4 Material properties

In developing models for the erosion of brittle materials, it is important to know the basic fracture parameters. This usually involves knowing at least the following: (a) moduli and Poisson's ratio, (b) K-V diagram where K is the stress intensity factor and V the velocity, (c) the critical stress intensity factor, K_{Ic}, (d) fracture surface energy, (e) maximum crack velocity, (f) yield strength, and (g) hardness. Ideally it is also useful to know how the above properties vary with (a) temperature, and (b) strain rate. Techniques and expertise are available in the laboratory for measuring the above parameters. As described later, studies of the effects of environment and temperature on the strength and toughness of zinc sulphide (ZnS) are in progress.

1.5 Solid particle impact

It is frequently useful to know how a material responds to solid particle impact. Studies of this nature are also in progress in the laboratory. Gas guns are available for projecting either (a) specimens at suspended particles or (b) particles at specimens. Velocities up to about 1000 m s-1 can be readily achieved. Apparatus is also available for multiple impact studies; specimen temperature can be varied from liquid nitrogen temperature up to about 1000 K (see Andrews et al. 1983).

1.6 High strain rate properties

The high-strain rate properties of materials are of prime importance in impact situations. We have developed apparatus based on a miniaturised Hopkinson bar. The specimen and Hopkinson "bars" are all of millimeter dimensions. Advantages of the system are (a) that very high strain rates can be studied (the smaller the bar diameter potentially the higher the strain rate which can be tested), and (b) the chosen configuration allows specimens of high hardness to be studied (this is a serious limitation with most conventional Hopkinson bar arrangements). Strain rates up to 10^5 s^{-1} can be achieved.

1.7 Theoretical

Over the last decade we have mounted a considerable theoretical effort into liquid/solid impact problems. In collaboration with Professor M.B. Lesser (K.T.H. Stockholm, Sweden) we have studied (a) the mechanics of the production of high-speed liquid jet (Field & Lesser 1977), and (b) developed a geometric wave theory of liquid impact (Lesser 1981, Lesser & Field 1983a, 1983b). Matthewson has produced analytic solutions for the protection offered by thin elastomeric coatings (Matthewson 1979, 1981, 1982) and van der Zwaag and Field have produced finite element solutions for the protection offered by thin layers of hard/high modulus coatings. Finally, van der Zwaag and Field (1983) and Hand (1987) have used flaw models to predict strength degradation of a brittle material when subjected to liquid impact.

STATEMENT "A" per D. Tyrell
AFOSR/XOTD ([redacted])
TELECON 2/16/90 CG

2. PROGRESS

2.1 Equivalent drop size data

(a) Introduction

In rain erosion the potential for damage from any one particular drop is dependent on its size. It is therefore of particular importance to know what drop diameter any jet produced by the Cavendish single jet impact apparatus is equivalent to.

Equivalent drop size curves for the liquid jet apparatus were obtained by Rickerby (1976). In this exercise only high velocity data were obtained. Curves were fitted to this data and were extrapolated to extend the correlation to low velocities. This low velocity jet/drop correlation (Rickerby, 1976) is dubious due to questionable assumptions in the extrapolated of the original data (van der Zwaag, 1981; Hand, 1987).

The correlation method used by Rickerby (measurement of the diameter of the central plateau region of impact sites on perspex) is only applicable to normal impact. As many aircraft components are mounted at an angle to the forward direction angled impact is an important feature of the observed liquid impact phenomena. A new correlation method has therefore been developed which is applicable to both normal and angled impact.

(b) Drop Impact

Normal and angled drop impacts were undertaken using a large bore gas gun developed in this laboratory by Blair (1981). Perspex samples were mounted in polythene sabots and fired at water drops suspended on carbon fibres. The water drop was protected from the air blast in front of the sabot by paper screens which the sabot penetrated before hitting the drop. Following impact the sabot was brought to rest by a catching tube system.

(c) Measurement of damage area

Following either jet or drop impact surface profile measurements were taken of the impacted samples using a modified Talysurf surface profilometer. The samples were mounted on a micro-computer controlled x-y stage: this allowed the sample to be scanned in two dimensions generating data about an area of the surface, rather than the linear data obtained with a conventional Talysurf. The data is collected via the micro-computer and is written on a floppy disc. This data was subsequently transferred to the university mainframe computer to produce contour and surface plots such as those shown in Figure 1.

The limits of the damaged region were estimated on the contour plots and the area of this region was measured using a planimeter. The major uncertainty in these measurements was in determining the limits of the damaged region from the contour plots: the planimeter gave results that were repeatable to 1% or better. On average the

error in the measured areas was about 5% although in extreme cases it could reach 10%.

The new equivalent drop curves for the 0.8 mm and 1.6 mm diameter nozzles are shown in Figure 2. We now have much more confidence in this data at low velocities.

2.2 Fracture strength of various zinc sulphide specimens

The fracture stress of zinc sulphide with different surfaces was measured using the hydraulic pressure test technique. Four sets of samples were examined in this particular study: Barr & Stroud "test material" (batch 1); British Aerospace Stevenage material (batch 2); samples roughed to size by Barr and Stroud and finished by Vintons (batch 3) and samples processed by Barr and Stroud to RSRE Malvern specifications (batch 4). The samples were all visually similar and were in the form of 25 x 2mm discs.

(a) Fracture stress

The radius at which fracture occurred, the fracture stress at the point of fracture, the equivalent flaw size, the stress at the centre of the disc (i.e. the maximum stress the disc supported) and from that the maximum flaw size in the central region are given in Tables 1-4.

The average fracture stress is low compared to previous data (Hand 1987) and the results show considerable scatter. The stress measured at the central region was often significantly higher than the stress at the point of fracture showing that the maximum flaw size was not uniform across the specimen.

(b) Liquid impact

Liquid jet impact at a velocity sufficient to cause visible damage can be used as a qualitative tool to detect any gross flaws in the surface. A typical damage mark in a brittle solid is made up of many short circumferential cracks. These are formed at defects (flaws) as the Rayleigh surface wave propagates out from the impact site. The cracks are short because the stress wave forming them is of short (sub-microsecond) duration. The crack patterns in Figures 3, 4 are typical for zinc sulphide which has had a good surface finish. The presence of long linear cracks is invariably an indication that grinding damage has not been adequately removed by subsequent polishing (van der Zwaag and Field, 1982). Such linear cracks are clearly visible in Figures 5-9. On the one specimen from each batch allocated to this test, large flaws were discovered in all cases except from the material processed by Barr and Stroud to RSRE specifications where a typical liquid impact site was observed (see Figures 3,4).

(c) Grain size

Examination of the specimen surface after etching in bromine and ethanol shows a maximum grain size of about 4 μm in all cases. This is significantly smaller than the

preferred grain size of 8 μm which has been shown to maximize the fracture toughness of zinc sulphide (Field, van der Zwaag and D Townsend), but is of the same order as for other specimens tested.

(d) Conclusions

The material supplied is not as good as that tested on previous occasions. Fracture stress measurements indicate large flaws which can be revealed by high velocity liquid impact. These flaws are most likely formed during grinding and have not been completely removed by polishing. Greater care at this stage would produce material with strength greater than 100 MPa.

2.3 Coated and ion-implanted zinc sulphide

These results were obtained on Purchase Order F6170887W0948 and are included here for completeness. In all cases the samples were in the form of 25.4 mm diameter 2 mm thick discs. They were impacted by liquid jets fired from a 0.8 mm orifice nozzle. Each specimen point represents 5 impacts at the centre of the disc. The "residual" strength curves were obtained following the procedure outlined in detail above in section 1.2. The substrate for the coated and ion-implanted specimens was Raytheon low defect polish material.

(a) Raytheon low defect polish

The results are given in Table 5 and are plotted in Figure 10. The plateau value was obtained by using the three unimpacted specimen values with strength in excess of 90 MPa and the three values at 115 m s^{-1} which showed no strength loss. The plateau value is 94 ± 5 MPa. The threshold value is 115 m s^{-1}. Two points, labelled A and B, were not used since they gave non-central fracture origins. This is usually an indication of a major defect, for example left by grinding, which has not been properly removed by subsequent polishing.

The value of 94 ± 5 MPa is reasonably high. Other sources of ZnS, polished to different specifications, have had mean values in the range 60 to 100 MPa.

An impact by a jet from a 0.8 mm orifice 115 m s^{-1} is equivalent to an impact by a 6.5 mm diameter drop. This is based on a recent calibration using our latest nozzles by Hand (1987) and discussed in Section 1.3.

It is possible to calculate the threshold velocity for a nominal 2 mm diameter drop by using the equation.

$$(V_1/V_2) = (d_2/d_1)^{1/3} \qquad (1)$$

where V_1 is the measured threshold velocity, d_1 the equivalent drop size, V_2 is the required velocity and d_2 equals 2 mm. This gives V_2 a value of 170 m s^{-1}.

(b) OCLI coated ZnS

The results are given in Table 6 and are plotted in Figure 11. In all other cases, three experiments were performed at each velocity. The plateau value of 134 MPa is the mean of the three experiments at 125 m s^{-1} and the unimpacted results. The threshold velocity is taken as 120 ± 5 m s^{-1} since although there is one high value at 125 m s^{-1} the other two points are less than the plateau value.

This particular coating increases the plateau strength value, presumably because it adds compression. However, the improvement of the threshold value is only marginal. A value of 120 m s^{-1} for impact with a 0.8 mm jet is equivalent to a threshold value of 180 m s^{-1} for a nominal 2 mm diameter drop.

(c) Raytheon treatment and surface finish

The results are given in Table 7 and are plotted in Figure 12. The samples showed some noticeable handling damage (an example is given in Figure 13) which caused a large spread in the fracture stresses of both the impacted and the unimpacted specimens. Towards the top of Figure 13 we see part of the damage mark associated with a 200 m s^{-1} impact from a 0.8 mm jet. The central undamaged area and the associated short circumferential cracks are typical of liquid impact. However, the long linear crack labelled A is almost certainly due to grinding damage which has not been removed by adequate polishing. The long cracks in the lower half of the figure were associated with the surface scratches at the positions, labelled S, and were typical of damage found on many of the samples. Note that the cracks labelled B and C are again long and linear. The damage in the lower part of the figure is much further out from the impact site than would have been expected for this velocity impact, showing that the scratches significantly weakened the material. The plateau value of 85 MPa ± 27 MPa was calculated from the discs impacted at 125 m s^{-1} and below excluding the points labelled in the Table A (edge failure) and B (low strength NCF). The coating appears to have had a marginal effect. The plateau value is essentially the same as the Raytheon low defect polish material. The threshold velocity is slightly higher at 125 m s^{-1} (for a 0.8 mm jet). Three specimens achieved strengths in excess of 100 MPa compared with one of the low defect polish material. The overall performance was affected by grinding and handling damage.

(d) Yttria coating

The results are given in Table 8 and are plotted in Figure 14. The plateau value of 114 MPa was obtained from the 4 unimpacted specimens and the 3 specimens impacted at 125 m s^{-1}. The threshold velocity for strength reduction was 130 m s^{-1} and coating failure occurred above 140 m s^{-1}. The samples were provided with some handling damage in the form of surface scratches but this did not noticeably affect the data. As Table 8 shows there were 9 samples which had strengths exceeding 100 MPa. This suggests, as with the OCLI coating, that the treatment adds compression to the

substrate. The nature of the coating failure was unusual. Figure 15 includes two views (different illumination conditions) of the same fracture. The linear defect is typical of grinding damage. The centre of the impact site is to the left so that liquid flowed in the direction of the arrow (Figure 15b). As we have shown in earlier studies, there is a surface step across such cracks. The Yttria coating has detached relatively easily giving the long finger-like damage pattern. Figure 16 shows that coating failure can extend over very large distances. The centre of the impact, at 140 m s^{-1}, is at the point labelled A. This is surrounded by an area, labelled B, where the flowing liquid has removed the coating. From this region a long snake-like feature of coating failure, labelled C, extends to the edge of the specimen, labelled D. It's appearance suggests that the coating was in a state of tension and that once failure started it grew to the specimen edge. Figure 17 shows a V-shaped area where coating had detached. The circular feature we suggest is caused by the coating failure starting at one end of the V and then sensing the other end. It is clear that the Yttria coating, once it fails, does so in a spectacular fashion.

(e) Ion-implanted

The results are given in Table 9 and plotted in Figure 18. The plateau value of 145 MPa was obtained from the 2 unimpacted specimens and the 2 specimens impacted at 125 m s^{-1}. This value is significantly greater than for previous treatments because of the compressive stresses put into the surface by the ion-implantation which is also the reason for the sample "bowing-out" on the tested side. The threshold velocity of 125 m s^{-1} was clear despite the lack of samples and the severe scratching around the clip marks at the edge of the discs (see Figure 19). The samples also displayed a large variation in the discolouration produced by the implanting process.

(f) Plessey coated material

Experiments have also been completed on this material and reported in a Confidential Report to Dr J.A. Savage. Further research is planned.

(g) Conclusions

The OCLI and Yttria coatings appeared to add compressive stresses and an encouragingly large number of samples had strength in excess of 100MPa. However above 140 m s^{-1} the Yttria coating failed in a spectacular fashion (Figures 16 and 17). The Plessey coating showed exciting possibilities, but some aspects of the behaviour need further discussion. The Ion-implanted material gave very respectable strengths including one value of 176 MPa. Further work on this material would be of interest.

According to our latest calibration curves a jet from a 0.8mm nozzle at 125 to 130 m s^{-1} is equivalent to a 6mm spherical drop (see Figure 2). Nominal 2mm drop thresholds can be estimated from the formula given earlier. This gives a velocity of ca.180 m s^{-1}. The coatings do not increase the threshold velocities of uncoated material by more than a few m s^{-1} except for some of the Plessey material (and more work is

needed here). In general, it is difficult to increase threshold velocities for liquid impact for various reasons. (i) As impact velocity increases, the shock velocity in water (and hence the pressures) increase at a faster than linear rate. (ii) As impact velocity increases, the pulse duration, and area over which high pressures develop, both increase. Both these factors allow a wider range of flaws to be sampled and propagated. Significant improvements will only be possible if strong coatings, well bonded to the substrate are used.

There were several cases where (i) grinding damage had not been adequately removed and (ii) handling damage (Figures 13 and 19) had been added. This meant that the full potential of the specimens was not achieved.

2.4 High temperature measurements on zinc sulphide

Our work in this area uses the so-called Brazilian test geometry in which a disc is stressed diametrically in compression. Tensile stresses develop on the central axis which are related to the specimen geometry and applied load. The advantages of the test are that it uses small samples (the disc diameter is typically 10 mm and the specimen thickness 2 to 3 mm) and it is relatively easy to build a chamber around the specimen for control of environment and temperature.

Initial work by Hand (1987) showed an increase in strength with temperature up to about 100°C and then a linear decrease. The strength at 500°C was close to the room temperature value. However, a relatively small number of samples was available for the preliminary work. A new batch of 140 samples is currently being used to make the data more statistically significant and to extend the temperature range from -40°C to 600°C. During the period of this contract a new chamber has been designed and tested. The chamber can have the pressure lowered to ca. 10^{-3} Atm. The usual procedure is to pump down and flush out with nitrogen twice before stressing a sample.

The work is laborious since the specimens have to be heated and cooled slowly in an inert environment of nitrogen. At the higher temperatures, only two specimens a day can be analysed. The experiments should be completed by January 1989.

2.5. Effect of environment of the K_{IC} of zinc sulphide

The method selected for this work was the double torsion technique which has a geometry (shown in Figure 20) that makes K_{IC} independant of crack length. This results in a constant crack velocity for a fixed load and a crack velocity which can be calculated from the load relaxation in the case where the crossheads of the testing machine are at a fixed displacement. Both of these techniques need to be used to cover the whole range of velocities over which stress corrosion occurs. In initial work with this technique, (for example Wiederhorn, Evans and others) specimen grooving was recommended to help "channel" the crack. This approach though has serious disadvantages in that the crack moves from one side of the groove to the other and can

have it's motion perturbed. It is much better to take care with the precursor crack, since if a crack nucleates in the correct direction it usually continues satisfactorily. The procedure we use is to add a small notch at one end with a diamond saw. A knoop indenter is then moved from the notch a few millimeters to add a surface scratch. This causes the crack to follow that path rather than any of the microcracks put in by the process of sawing the notch. If the fittings are carefully aligned on the apparatus the crack will then proceed down the centre of the sample as desired.

2.6 Fracture toughness and hardness of zinc sulphide as a function of grain size.

A paper based on this research had been submitted to J. Mater. Sci.

2.7 Angled impact

A paper describing the theory of angled impact is being prepared and will be forwarded shortly. Experiments are in progress to develop a set of "equivalent drop" curves for angled jet impact with the Cambridge apparatus.

3. The Multiple Impact Jet Apparatus

3.1 Introduction

The Multiple Impact Jet Apparatus (MIJA) has been designed primarily for *multiple* water jet impact research, although obviously, it has a common basis with the single impact work that has gone before and still currently being undertaken. Whereas the single impact technique is capable of attaining high jet velocities for a small number of impacts per specimen, MIJA may be used for large numbers of repeated and reproducible impacts; albeit at more modest velocities. MIJA, therefore, both complements and supplements the single impact technique. Moreover, the range of velocities attainable by MIJA more than covers the 223 m s^{-1} (500 mph) used by the RAE Farnborough "whirling-arm" rain erosion rig which, it is anticipated, it could eventually replace.

The design details, manufacture and preliminary results of MIJA have been the special subject of a thesis (Davies 1988), A description of the development of MIJA and some early results was given in Davies and Field (1987). Experimental work undertaken using MIJA subsequent to the submission of the thesis, includes: rain damage assessment tests on rotor blade elastomeric coatings and various high modulus, hard coatings on ZnS. This work is still in progress and is outlined below.

3.2 Surface profilometry

MIJA can derive surface profile data, using "Talysurf" profilometer as outlined in section 2.1c above.

Modes of material deformation

Figure 21 shows a typical depressed annular damage region caused by drop impact on polymethylemethacrylate (PMMA). This damage was obtained using MIJA, from 25 impacts of 0.6 mm (4 mm diameter drop equivalent) jets at 150 m s^{-1} (a velocity chosen to be below the single impact visual damage velocity threshold). During multiple impact, incipient damage, or even possibly inhomogeneities in the surface material, enhance or inhibit the target response (deformation and fracture) from later impacts. This is borne out in Figure 21. Instead of a uniform circular depression usually caused by higher velocity single impacts, the height contours distinctly show, not only an oblate shaped damage site, but also several constricting 'bridges' across the annular depression. Note that the annulus appears to caused by compaction rather than displacement of material.

At higher multiple impact velocities many cracks are preferentially extended interacting in a three-dimensional manner to cause uplifting of 'blocks' of material. Figure 22 shows the effects of increased impact velocity and the effect of partially overlapping damage sites on perspex. Site A was formed by 25 consecutive 0.6 mm

jet (4 mm drop) impacts at 150 m s^{-1} (and was originally similar to the site shown in Figure 21). This was followed by similar sequences at 175 m s^{-1} on site B and 200 m s^{-1} at site C. It is clear from the increasing volume of raised material (from A → B → C) that this form of brittle damage is a precursor to erosion.

3.3 MIJA damage threshold studies on brittle materials

This differing nature of multiple impact on brittle materials is a major part of planned work using MIJA and to this end, some preliminary work [Davies & Field, 1987] has already been done. Analysis of the fracture surface of the deep cracks (figure 24), shows regular, incremental crack growth features — circumferential discontinuities. The scalloped edges (s) of the broken specimen indicates that the fracture surface is made up of several overlapping cracks, making measurement difficult, but the growth features are visible on each section. They appear almost equi-spaced for approximately 60% of the specimen thickness. Further down the spacing increases, with only 2 or 3 marks being visible over the final millimetre.

Other interesting features are also apparent. The interaction of overlapping cracks, are visible as discontinuity lines, running from top to bottom of the fracture surface. These were just visible inside the impact damaged, but unbroken specimen, as white lines. Further deep cracks (c &c') are visible.

Comparative study of five coated ZnS specimens

Six 25 x 25 x 3 mm^3 ZnS specimens were obtained, from RAE Farnborough five of which had been specially prepared on one face with a thin layer of proprietary, high modulus, rain-erosion resistant material. The sixth, uncoated specimen acted as a 'control'. Each of the specimens, from either Vinten, Balzer or OCLI, have been subjected to the standard rain erosion conditions of the RAE Farnborough whirling arm rig over a 19 x 19 mm^2, until erosion weight-loses were recorded. For five specimen the erosion time was 21 minutes, roughly equivalent to 55 impacts/mm^2, but one coated specimen (Vinten) required only 15 minutes, 40 impacts/mm^2.

A 3 mm (triangular) section of each specimen, viewed in transmitted light, can be compared in Figure 23. Their appearance are clearly not quite as random or chaotic as might have been expected, for within the mass of overlapping impact sites, clearer regions are distinctly visible. Despite the more obvious similarities, each has distinctive, differences. Photographic enlargements and low-powered microscopic examination of the specimen permitted the approximate measurement of the clear zones, in order to determine possible 'characteristic diameters'. A minimum of fifty measurements were recorded for each 'randomly-picked' specimen and these results are graphically summarised in Figure 25.

The uncoated material has a uniform distribution of clear sites with a mode at the scaled diameter of 8 mm (0.38 mm on the specimen). The coated specimens, on the other hand, have distributions which fall into one of the following two categories:

(1) the same mode at 8 mm (0.38 mm), but have few or no sites below this value — both Balzer specimens fall into this category,

(2) similar to the uncoated material, but with a mode that is increased to a diameter of 10 mm (0.47 mm) — both OCLI specimens fall in this category

The single specimen from Vinten appeared to have both of these attributes, yielding a modal site count at 10 mm (0.47 mm) *and* a distribution exhibiting the reduced number of sites below this value.

The clear zones are caused by the first few damaging impacts onto the specimen surface. Single impact studies on ZnS have shown that circumferential damage cracks occur with a reasonably uniform radial distribution of lengths and depths; starting small, gradually getting larger and reaching a maximum before eventually diminishing. Multiple impact studies on the same site, using MIJA, have revealed that it is the **longer** cracks that are extended deep into the material. (The random nature of the impacts ensures that it is not necessarily all the longest cracks that are extended the furthest).

The critical diameter d_c for a 2 mm water drop of radius R impacting a rigid target at a velocity V of 223 m s^{-1} is approximately given by:

$$d_c = \frac{2\,R\,V}{C},$$

$$= \frac{2\,R\,V}{C_0 + 2V} = 0.23 \text{ mm}$$

where C is the shock velocity and C_0 the acoustic velocity for water.

This is equivalent to about 4.8 mm on the enlarged (x21) images of each specimen. By inspection of the graphs in Figure 25 it seems that only the 'uncoated' specimen has a high number of clear zones with this particular diameter. The circumferential fracture zones of each coated specimen shows obvious signs of modification — the positions of their longest multiple impact extended cracks has been moved further out from the centre of impact.

3.4 MIJA random impact studies

Significant steps have been taken, with the introduction of MIJA, towards being able to emulate the drop impact erosion produced by the RAE Farnborough 'whirling-arm' rig, using the jet technique. The main difference in the damage between the two techniques is expected to be due to the unique ability of MIJA to repeatedly simulate the same equivalent drop size each time it is fired.

Unfortunately, to present similar statistics to those above would require approximately 20000 impacts, which with the present MIJA (an imporved model is being developed) would take upwards of four working days for each specimen. As an indication, merely of the similarity of the damage caused by the two techniques, a MIJA random impact sequence of 50 impacts/mm^2 on uncoated ZnS is shown in Figure 26. The larger (4 mm) equivalent drop size used on MIJA has caused somewhat deeper fracturing, but it is essentially the same sort of damage — including, notably, the characteristic 'clear' zones.

Single impact studies on OCLI coated samples (section 23b) suggests that the coating adds compression to the substrate ZnS. This is consistent with the results of Figure 25. The threshold value obtained from the single impact work was 180m s^{-1}. Results using MIJA with a 0.6mm jet (equivalent to a 4mm drop) and impacts in excess of 100 obtained a threshold velocity of ca. 150 m s^{-1}. When the conversion formula was used (equation 1 in Section 2.3) an unetched velocity of 188 m s^{-1} was found, the agreement with the single impact curve is excellent.

References

Andrews, D.R. Walley, S.M., Field J.E.	Solid particle erosion studies in the Cavendish Laboratory.	Proc. 6th Int. Conf. on Erosion by Liquid & Solid Impact (ed. Field, J.E. and Corney, N.S.) Cavendish Lab. Cambridge (1983), Paper 36.
Blair, P.W.	The liquid impact behaviour of composites and some infra-red transparent materials.	Ph.D thesis,University of Cambridge (1981).
Davies, P.N.H., Field, J.E.	Multiple impact jet apparatus (MIJA): Development and some damage threshold results.	Proc. 7th Int.Conf. on Erosion by Liquid and Solid Impact, (ed. Field, J.E. and Dear, J.P.) Cavendish Lab. Cambridge (1987) Paper 7.
Field, J.E. Gorham, D.A. Rickerby, D.G.	High speed liquid jet and drop impact on brittle targets.	Proc. of ASTM Symp. on Erosion,Vail,ASTM, STP 664 (ed. W. Adler), (1979).
Field, J.E. Lesser, M.B.	On the mechanics of high speed liquid jets.	Proc. Roy. Soc. Lond.. A 357, 143-162, (1977).
Field, J.E. van der Zwaag,S. Townsend, D.	Liquid impact damage assessment for a range of infra-red materials.	Proc. 6th Int. Conf. on ELSI (eds. Field, J.E., Corney, N.S.), Cavendish Lab. Cambridge, (1983). Paper 21.
Field, J.E. Lesser, M.B., Dear, J.P.	Studies of two-dimensional liquid-wedge impact and their relevance to liquid-drop impact problems.	Proc.Roy.Soc. Lond. A 401, 225-249, (1985).
Gorham, D.A. Rickerby, D.G.	A hydraulic strength test for brittle samples.	J.Phys. E 8, 794-796, (1975).
Hand, R.J.	Impact & fracture properties of infra-red & optical transmitting materials.	Ph.D thesis, University of Cambridge (1987).
Lesser, M.B.	Analytic solutions of liquid-drop impact.	Proc. Roy. Soc. London. A 377 289-308 (1981).

Lesser, M.B. Field, J.E.	The impact of compressible liquids	Ann. Rev. Fluid Mech. 15, 97-122, (1983a).
Lesser, M.B. Field, J.E.	The geometric wave theory of liquid impact	Proc. 6th Int. Conf. on ELSI (eds. Field, J.E. Corney, N.S.), Cambridge, Sept.(1983). Paper 17.
Matthewson,M.J.	Theoretical aspects of thin protective coatings	Proc. 5th Int. Conf. on ELSI (ed. Field, J.E.) Cambridge (1979) Paper 73.
Matthewson, M.J.	Axi-symmetric contact on thin compliant coatings.	J. Mech. Phys. Sols. 29 (2), 89-113, (1981).
Matthewson, M.J.	The effect of a thin compliant protective coating on Hertzian coated stress.	J. Phys. D: Appl. Phys. 15, 237-249 (1982).
Matthewson, M.J. Field, J.E.	An improved strength measurement technique for brittle materials.	J Phys.E 13, 355-359, (1980).
Quinn, George D.	Delayed failure of a commercial vitreous bonded alumina.	J. of Mat. Sci. 22 2309-2318 (1987).
Rickerby, D.G.	High velocity liquid impact and fracture phenomena.	Ph.D thesis, University of Cambridge (1976).
van der Zwaag, S.	Liquid impact and contact damage in brittle solids	Ph.D thesis, University of Cambridge (1981).
van der Zwaag,S. Field, J.E.	Liquid jet impact on zinc sulphide	J. Mater. Sci. 17, 2625-36 (1982).
van der Zwaag, S., Field, J.E.	Rain erosion damage in brittle materials	Engineering Fracture Mech. 17 (4), 367-379, (1983).

TABLE 1 Zinc Sulphide fracture stress data batch1

fracture radius mm	fracture stress MPa	fracture stress at centre MPa	e f s microns	e f s at centre microns
2.5	74	79	76	67
2.5	81	87	64	55
4	86	100	57	42
5	59	85	122	58
4.5	54	69	145	87
8	49	91	171	51
2.5	55	59	139	122
5	70	85	86	57
2	93	96	48	46
2	103	106	39	37
3.5	81	90	64	51
5	50	61	168	111
4.5	42	54	239	145
4	57	65	127	98
2.5	99	106	43	37
5	72.4	88	80	54
3.5	47	55	194	141
1.5	54	55	145	138
5	45	55	205	138

Average fracture stress =67MPa (SD=19)

TABLE 2 Zinc Sulphide fracture stress data batch 2

fracture radius mm	fracture stress MPa	fracture stress at centre MPa	e f s microns	e f s at centre microns
3	93	100	48	42
1	84	85	59	58
2	114	118	32	30
5	78	96	69	45
4.5	98	115	44	32
2	119	124	30	27
2.5	71	75	83	73
5	88	108	55	36
2.5	62	67	109	93
3.5	89	100	53	41
6	79	108	68	36

Average fracture stress =91(SD=15)

TABLE 3 Zinc Sulphide fracture stress data batch 3

fracture radius mm	fracture stress MPa	fracture stress at centre MPa	e f s microns	e f s at centre microns
3.5	56	61	134	111
1.5	95	97	46	44
2	64	66	101	95
0.5	104	104	38	38
5.5	46	59	195	119
3	43	47	220	193
5	67	82	93	63
2	95	98	47	44
3	49	55	172	140
0.5	94	94	47	47

average fracture stress=71 (SD=23)

TABLE 4 Zinc Sulphide fracture stress data batch 4

fracture radius mm	fracture stress MPa	fracture stress at centre MPa	e f s microns	e f s at centre microns
2.5	120	126	29	27
2.5	96	104	45	39
7	48	82	183	63
0.5	100	100	42	42
0	43	43	228	228
2.5	84	89	60	53
2	82	85	62	58
4.5	97	114	45	32
6	78	104	70	38
2.5	93	97	48	44

Average fracture stress=84 (SD=24)

TABLE 5 Raytheon low defect polish Zinc Sulphide

impact velocity $m\ s^{-1}$	fracture stress MPa	fracture stress at centre MPa	e f s microns	e f s at centre microns
0	EDGE	FAILURE		
0 (A)	60(ncf)	100	117	42
0	96	100	46	42
0	92	95	50	47
115	93	96	48	46
115	89	93	53	48
115	103	103	40	39
120	62	63	109	107
120	61(ncf)	78	111	68
125	70	70	87	85
125	70(ncf)	94	85	47
125	55(ncf)	85	137	58
125(B)	47	58	191	126
125(C)	91(ncf)	122	51	28
125	51	51	159	158
140	48	56	180	134
140	58	59	127	119
140	62	65	108	98
150	60(vis)	60	117	115
150	56(vis)	57	133	130

ncf=non central failure

vis=visual damage

TABLE 6 OCLI coated Zinc Sulphide

impact velocity m s^{-1}	fracture stress MPa	fracture stress at centre MPa
0	91(ncf)	118
0	157	159
0	153	155
0	152	171
125	119	134
125	149	167
125	118	122
135	108	110
135	123	139
135	126	157
140	137	150
140	119	120
140	78	81
150	62	63
150	61	62
150	59	59
160	67	70
160	57	57

Equivalent Flaw sizes (EFS) were not calculated since there was no data on the stress in the substrate.

TABLE 7 Raytheon treatment and surface finish Zinc Sulphide

impact velocity $m\ s^{-1}$	fracture stress MPa	fracture stress at centre MPa	e f s microns	e f s at centre microns
0	64	71	102	84
0	70	70	86	86
0	128(ncf)	156	25	17
110 A	EDGE	FAILURE		
110	64	70	103	85
125 B	12(ncf)	57	(3007)	129
125	110	116	35	31
125	96	101	45	41
125	62	71	110	84
140	93	105	48	38
140	63	63	105	105
140	59	61	119	113
140	56	59	132	120
150	54(vis)	54	144	144
160	101	105	41	38
160	38(vis)	38	293	291
170	52(vis)	52	156	155
200	38(vis)	39	295	282

TABLE 8 Yttria cotaed Zinc Sulphide

impact velocity $m\ s^{-1}$	fracture stress MPa	fracture stress at centre MPa
0	119	122
0	73	82
0	106	108
0	116	124
125	130	134
125	116(ncf)	135
125	138	145
132	138	156
132	101	103
132	106(ncf)	124
140	62 (c)	63
140	81	86
140	75	76
160	79	82
160	43(c,s)	44
160	60 (s)	61
200	48(c,s)	48

c=Visual damage in the coating

s=Visual damage in the substrate

TABLE 9 Ion-implanted Zinc Sulphide

impact velocity m s^{-1}	fracture stress MPa	fracture stress at centre MPa	e f s microns	e f s at centre microns
0	EDGE	FAILURE		
0	EDGE	FAILURE		
0	113(ncf)	144	33	20
0	176	184	14	12
125	142	148	21	19
125	147	148	19	19
140	72	75	80	74
140	56(ncf)	104	131	39
140	78(ncf)	126	68	26
160	97	98	44	44
160	55	56	139	136

a

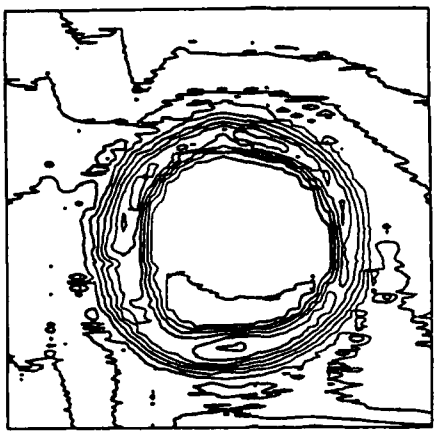

b

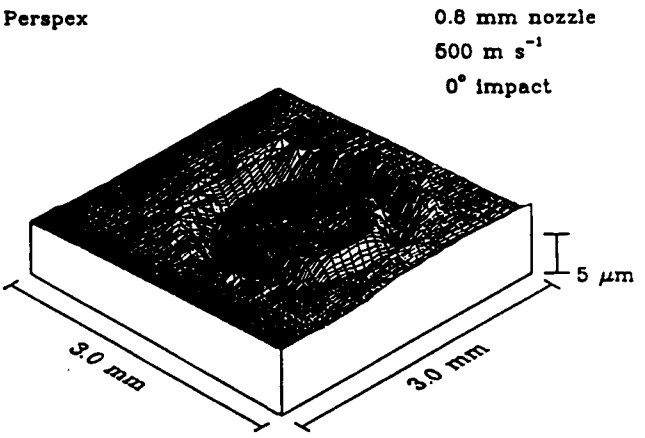

Figure 1: Contour and surface plots of a liquid impact damage site on perspex

a) Contour plot

b) Surface plot

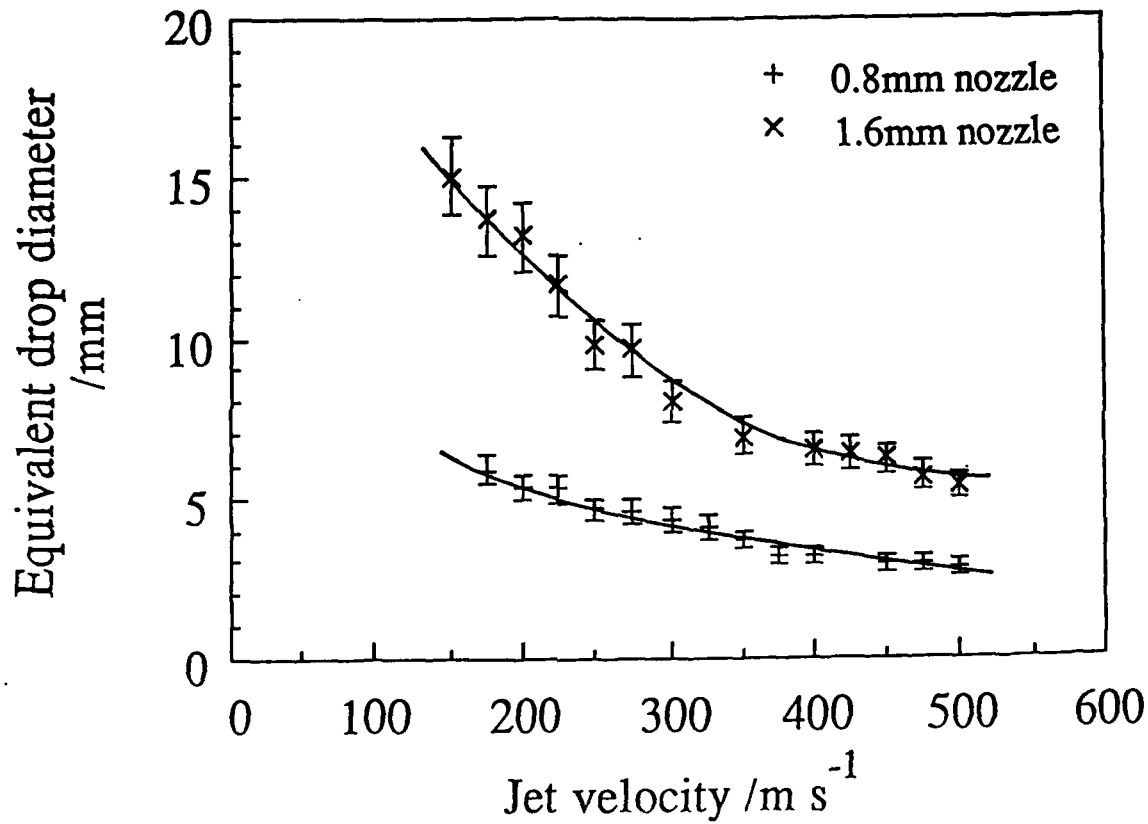

Figure 2: Equivalent drop size curves for the 0.8 mm and 1.6 mm diameter nozzles

FIGURE 3 BATCH 3

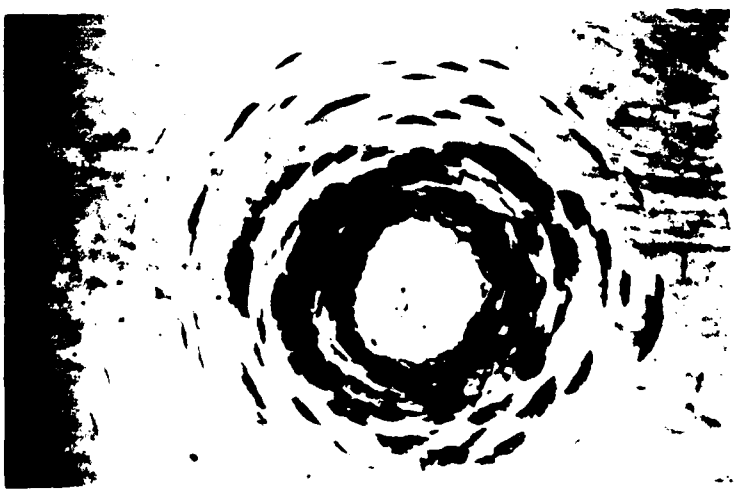

FIGURE 4 BATCH 4

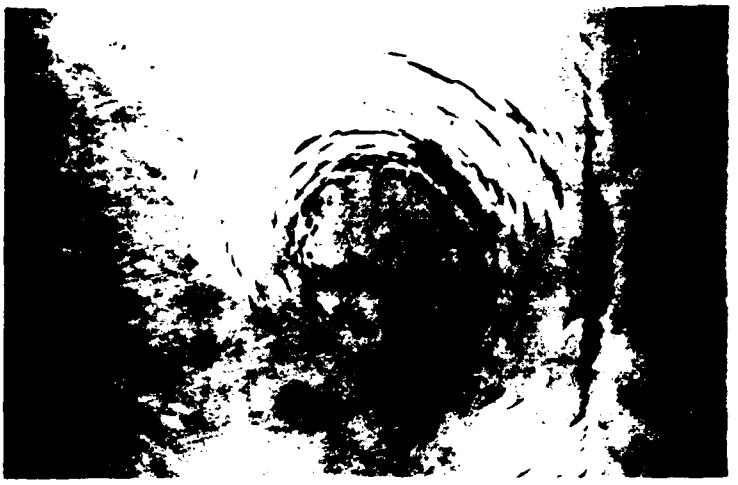

FIGURE 5 BATCH 1

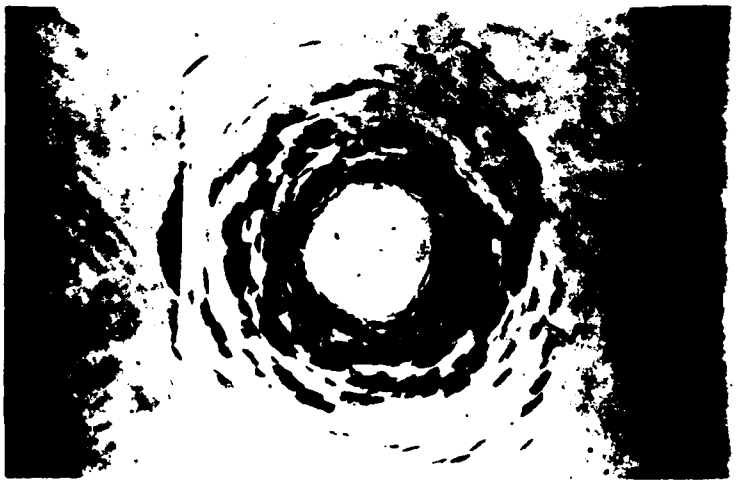

FIGURE 6 BATCH 3

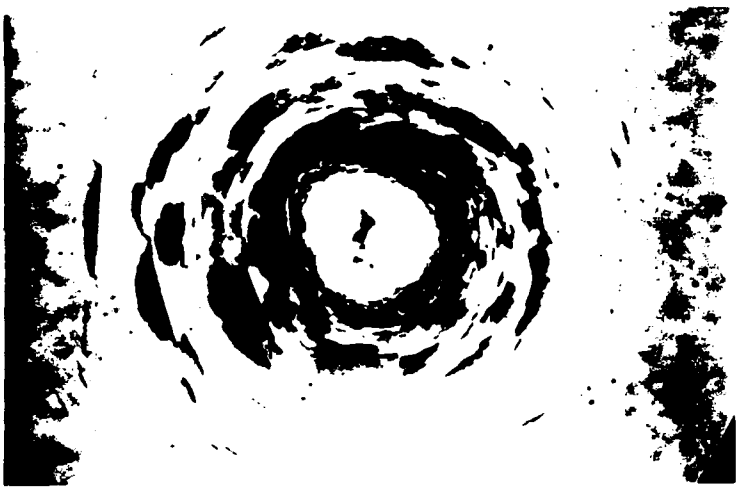

FIGURE 7 BATCH 3

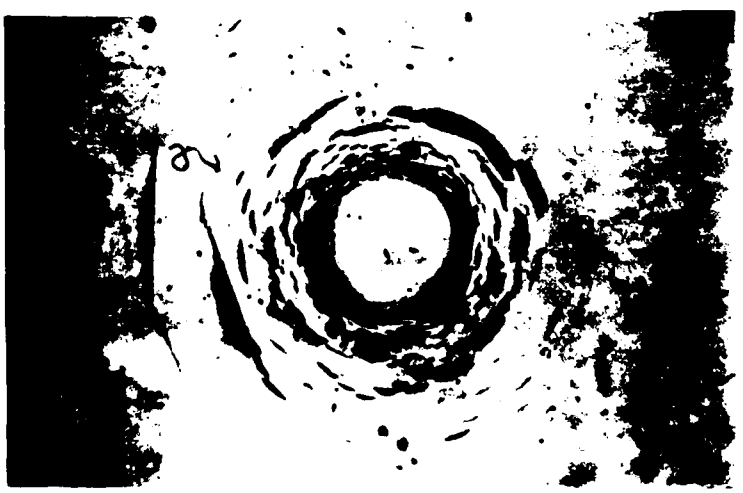

FIGURE 8 BATCH 2

FIGURE 9 BATCH 2

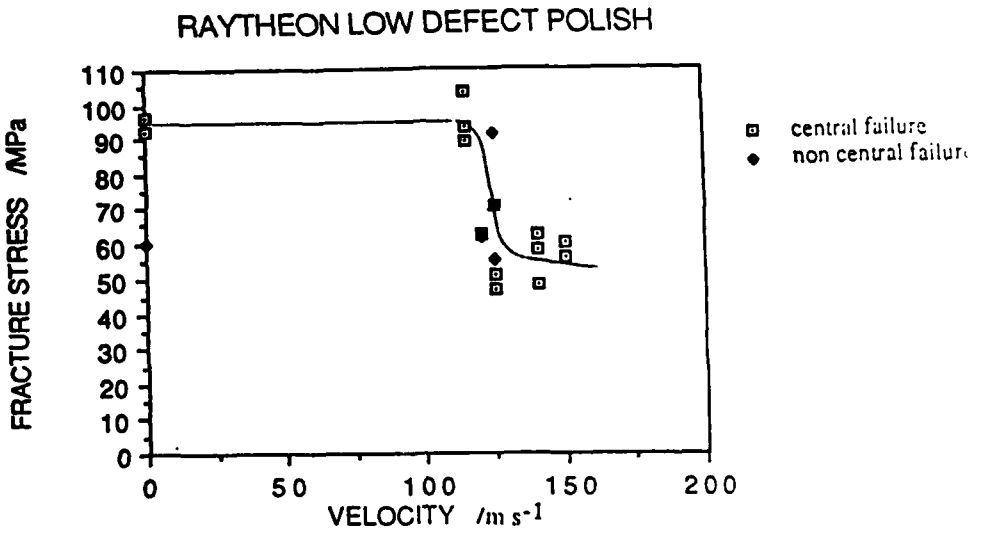

FIGURE 10

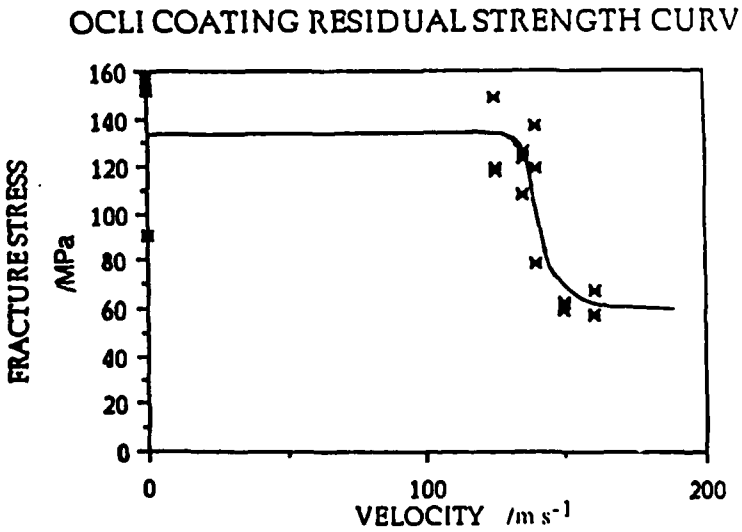

FIGURE 11

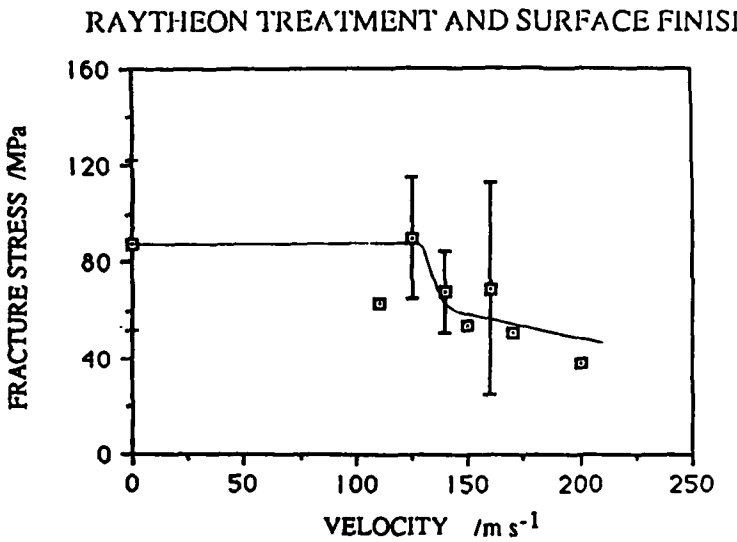
RAYTHEON TREATMENT AND SURFACE FINISH
FRACTURE STRESS /MPa
160
120
80
40
0
0
50
100
150
200
250
VELOCITY /m s-1

FIGURE 12

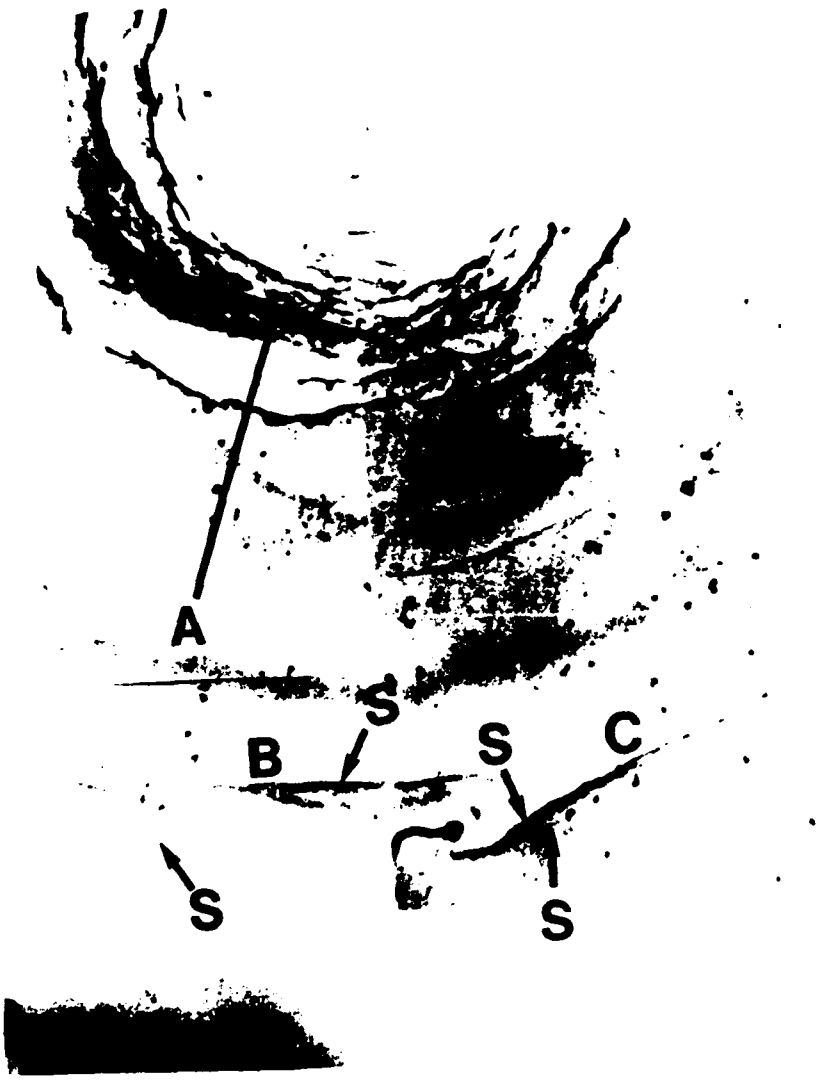

FIGURE 13

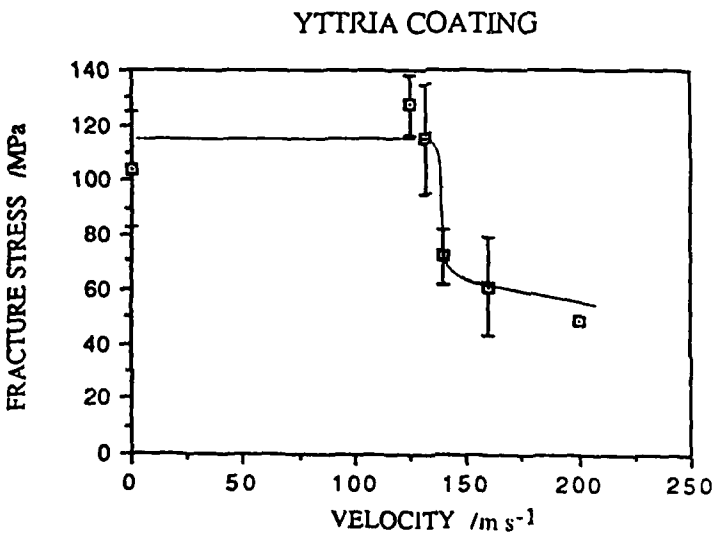
YTTRIA COATING
FRACTURE STRESS /MPa
140
120
100
80
60
40
20
0
0
50
100
150
200
250
VELOCITY /m s-1

FIGURE 14

FIGURE 15a

FIGURE 15b

FIGURE 16

FIGURE 17

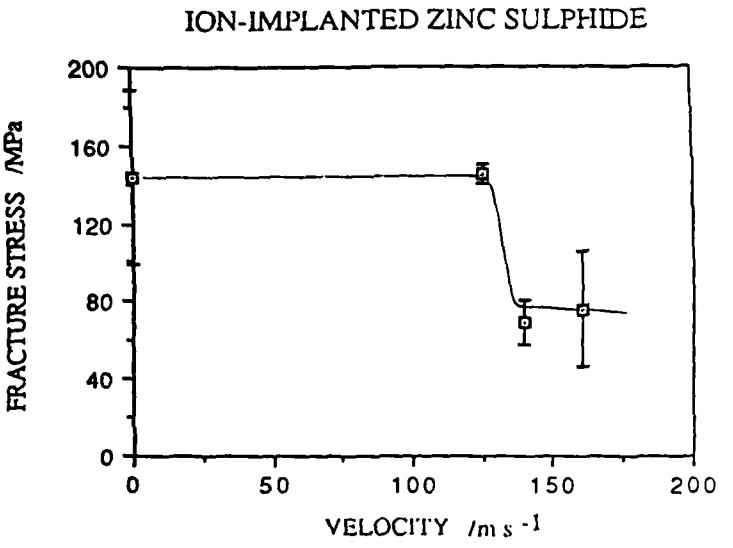
ION-IMPLANTED ZINC SULPHIDE
FRACTURE STRESS /MPa
200
160
120
80
40
0
0
50
100
150
200
VELOCITY /m s -1

FIGURE 18

FIGURE 19

DOUBLE TORSION APPARATUS

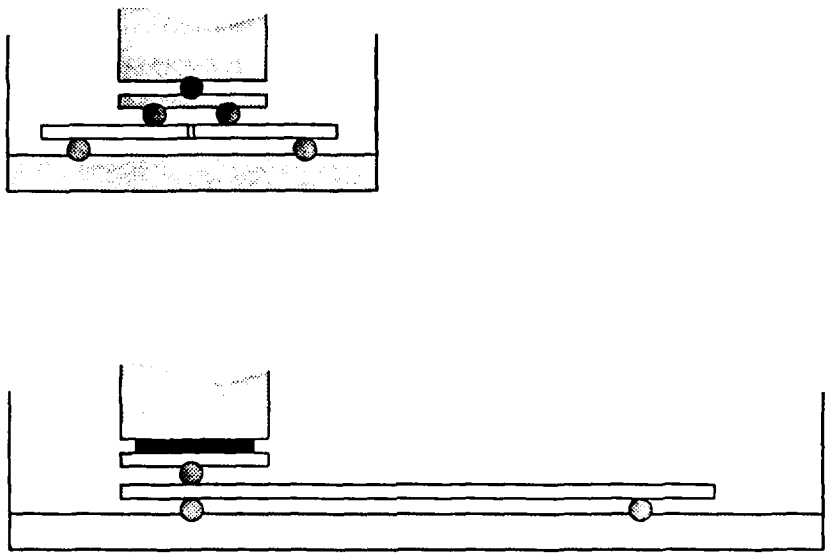

FIGURE 20

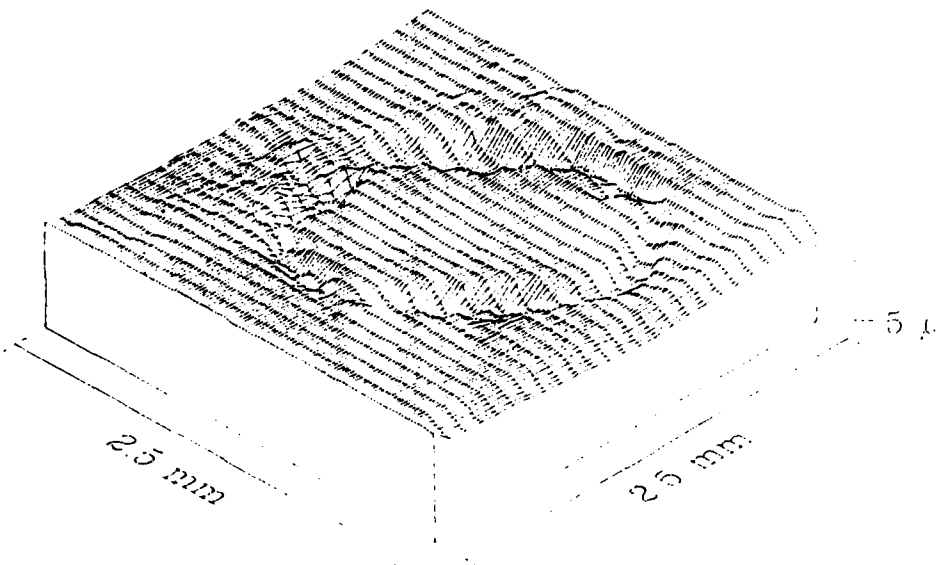

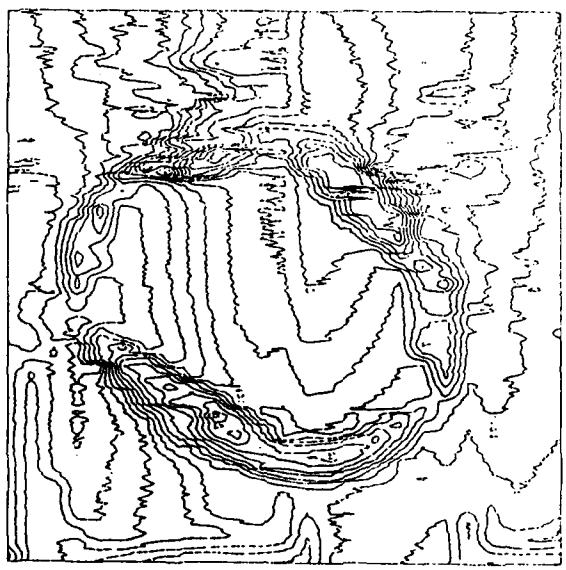

871019a
Perspex
0 mm jet
150 m s⁻¹
impact

0.5 mm

Fig. 21

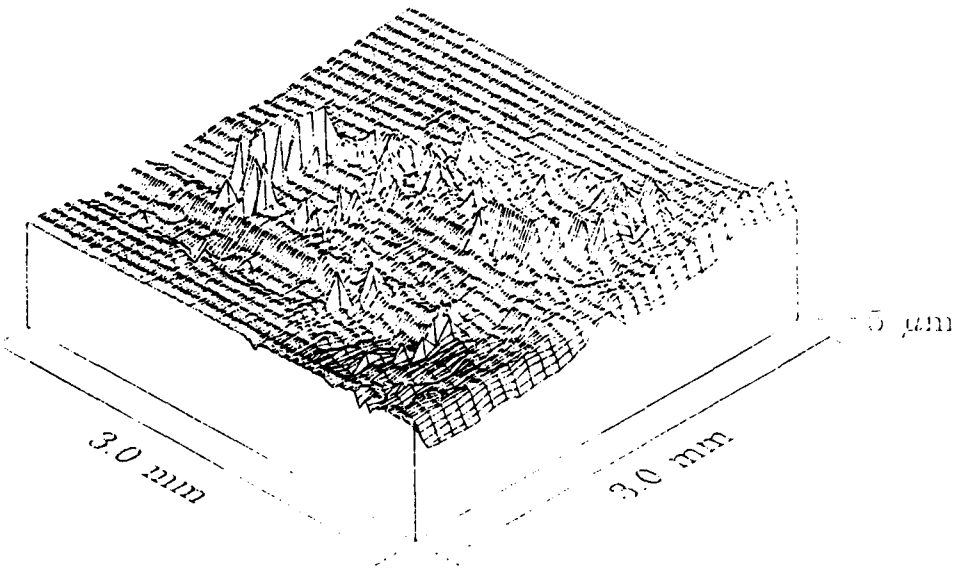

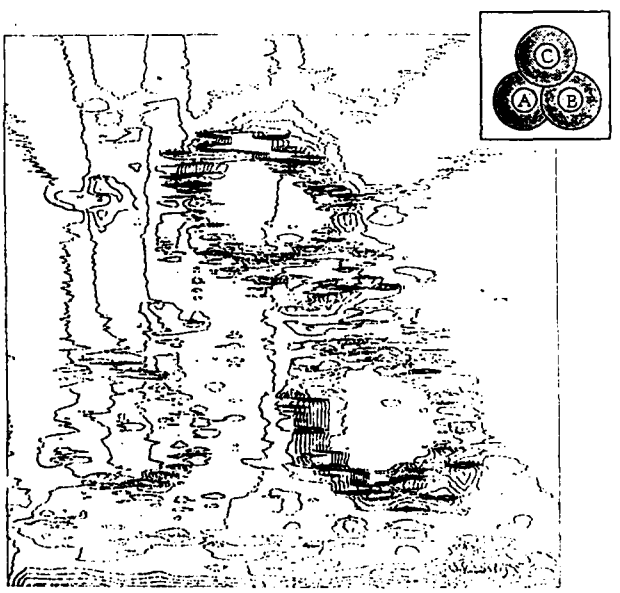

Fig. 22

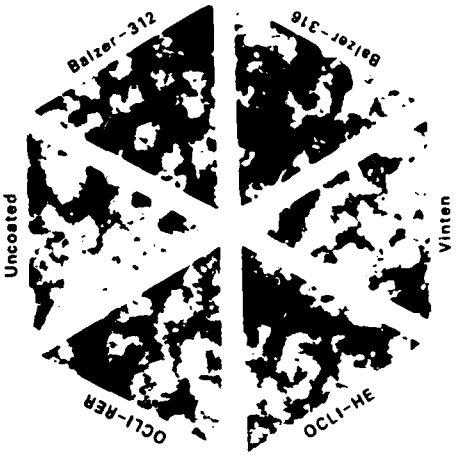

Fig. 23

Fig. 24

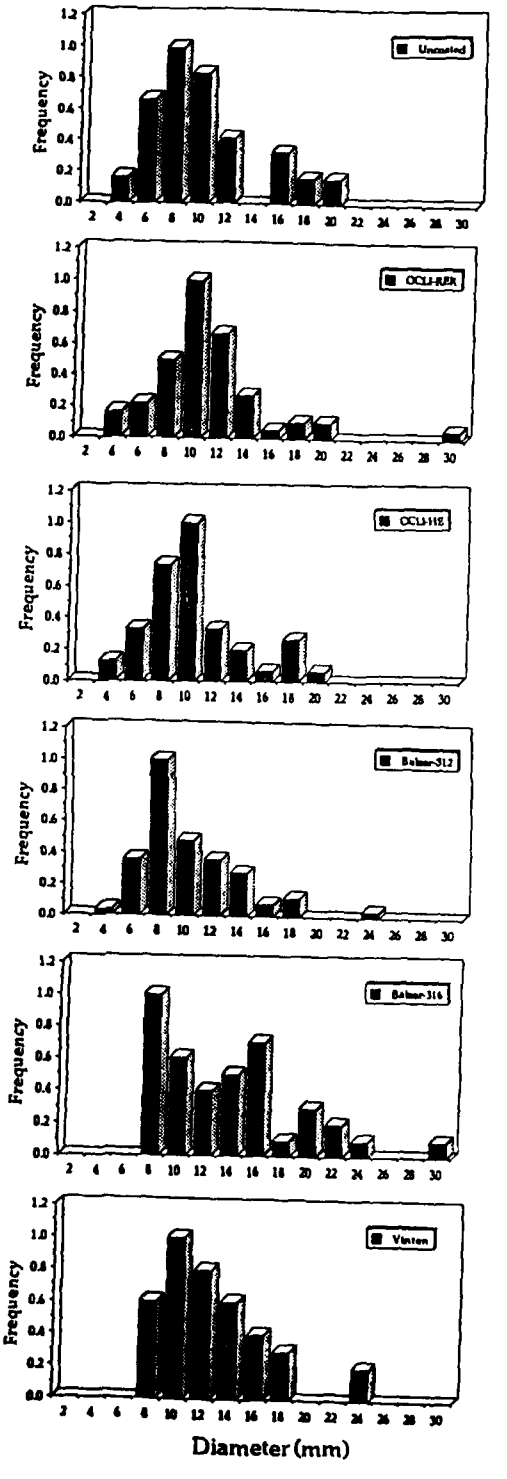
Uncoated
OCLI-HER
OCLI-HE
Balzer-312
Balzer-316
Vitron
Frequency
Diameter (mm)

Fig. 25

a

b

Fig. 26